

“Ideal” Engineering Alloys

Tianshu Li,¹ J. W. Morris, Jr.,¹ N. Nagasako,² S. Kuramoto,² and D. C. Chrzan^{1,*}

¹Department of Materials Science and Engineering, University of California, Berkeley, California 94720, USA

²Toyota Central Research and Development Laboratories Incorporated, Nagakute Aichi, 480-1192, Japan

(Received 15 July 2006; published 9 March 2007)

A newly discovered group of alloys, called Gum Metals, approaches ideal strength in bulk form, exhibits significant plastic deformation prior to failure, and shows no indications of conventional-dislocation activity. Two conditions must be met for a material to exhibit this “ideal” behavior: (1) the stress required to trigger conventional-dislocation plasticity in the material must exceed its ideal strength, and (2) the material must be intrinsically ductile when stressed to ideal strength. Gum Metals satisfy both criteria, explaining their remarkable mechanical properties.

DOI: [10.1103/PhysRevLett.98.105503](https://doi.org/10.1103/PhysRevLett.98.105503)

PACS numbers: 61.50.Lt, 62.20.Dc, 71.20.Lp

In 1926, J. Frenkel [1] suggested that the ideal strength of a metal should be given approximately by $\mu/5$, where μ is the metal’s shear modulus. Frenkel put forth the simple argument that plastic deformation would become inevitable when the applied shear stress was sufficient to make adjacent planes of atoms glide rigidly over one another. Since the yield strengths of typical metals were nearer $\mu/1000$, it was clear that the Frenkel model did not apply. Its major shortcoming was identified shortly thereafter [2–4] when it was realized that plastic deformation could be initiated by the motion of crystal dislocations at stresses well below the ideal shear strength.

The understanding of ideal strength has evolved significantly since the 1920’s [5–15]. The ideal strength of a crystalline solid is determined by the elastic instability of the crystal lattice, and the thermomechanical criteria that govern elastic stability are well established. However, very few bulk materials fail at the limit of strength.

Presently, researchers in the mechanics of materials are excited by the recent discovery of a group of high strength, ductile alloys, called Gum MetalsTM, whose bulk mechanical behaviors appear to be governed by elastic instability at the ideal strength [16]. Gum Metals are multicomponent body-centered-cubic (bcc) solid solutions based on the Ti-Nb binary (a typical composition is, in weight percent, Ti-35.9Nb-2Ta-2.7Zr-0.3O). These alloys sustain very large elastic deformation prior to yield ($\sim 3\%$ elastic strain). After yielding, at very high stress, they sustain significant plastic deformation prior to failure ($\sim 10\%$), apparently *without* the participation of conventional dislocations. The plastic strain occurs through the formation of large, planar faults, accompanied by “nanodisturbances” that can be represented as dislocation dipoles, but with non-lattice Burgers vectors [17]. This pattern of deformation might be expected of a material that fails in shear near its ideal strength. Prior studies of this behavior focus on the vanishing of certain elastic constants at a certain electron concentration [18,19]. Here, we formulate an argument that addresses the competition between dislocation mobility and ideal shear, and demonstrate that, in contradiction

to 60 years of metallurgical wisdom, it may be practically possible to pin dislocations even at stresses that exceed the ideal strength of the crystal.

There are two criteria that must be satisfied for a material to have useful strength near its ideal value. First, the ideal strength must be below the stress at which the material would deform by conventional dislocations. Second, when the material is stressed to elastic instability (ideal strength) it must fail by shear rather than by cleavage fracture, whatever the loading geometry. Consideration of the elastic properties of Gum Metals indicates that they satisfy both criteria.

The simplest approach to *ab initio* calculations of the elastic properties of disordered solid solutions is a pseudopotential-based virtual crystal approximation (VCA). Within VCA, the electron-ion interaction within the alloy is modeled using a pseudopotential that is the concentrated-weighted average of the pseudopotentials for the pure elements composing the alloy. VCA has the advantages of computational simplicity and preservation of the crystal symmetry of the alloy. The elastic properties of Ti-V alloys are described well within VCA, and these alloys will serve as a Gum Metal approximant.

The elastic constants of bcc Ti-V alloys are shown in Fig. 1 plotted versus the valence electron concentration, e/a . The theoretical values are calculated using ABINIT [20] with Troullier-Martins type pseudopotentials generated using the Fritz-Haber-Institute pseudopotential code [21] and applying VCA. An energy cutoff of 50 Ha (1360 eV) is necessary to obtain convergence. The Brillouin zone summations are carried out on a symmetrized $14 \times 14 \times 14$ Monkhorst-Pack grid. A Fermi-Dirac smearing (0.01 Ha) is used to accelerate convergence. Comparison of the results of VCA calculations for the shear modulus $C_{11} - C_{12}$ for Ti-V alloys to those computed using supercell methods [22] and experimental measurements [23] indicate that VCA provides a very good description of the elastic properties of the alloys (Fig. 1).

Figure 1 shows the computed moduli governing tension (E_{hkl}) and shear (G_{hkl}) for the three crystalline orientations

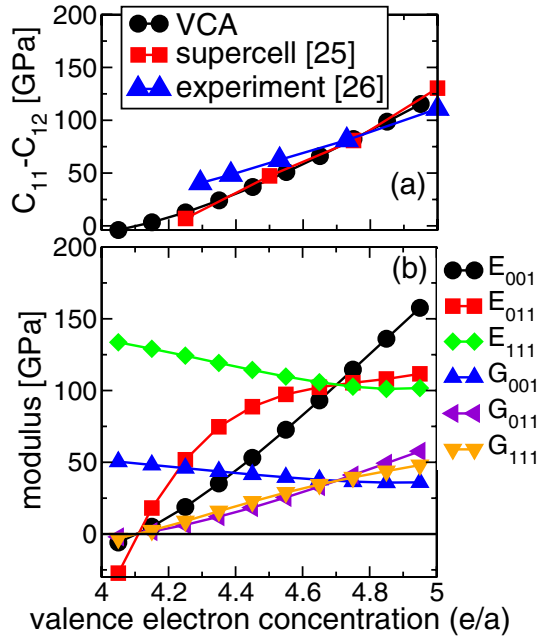


FIG. 1 (color online). (a) Comparison of experimental, supercell and VCA results for $C_{11} - C_{12}$. Supercell, VCA, and experimental results are in reasonable agreement, suggesting VCA provides an accurate description of Ti-V alloys. (b) Elastic moduli of bcc binary Ti-V alloys computed using VCA (see text).

of highest symmetry in the bcc lattice of Ti-V: $\langle 001 \rangle$, $\langle 011 \rangle$, and $\langle 111 \rangle$. E_{hkl} is the modulus for tension along $\langle hkl \rangle$, and the G_{hkl} 's are shear moduli with G_{001} corresponding to shear along $\langle 001 \rangle$ on $\{010\}$, G_{011} to shear along $\langle 011 \rangle$ on $\{011\}$, and G_{111} to shear along $\langle 111 \rangle$ on the planes $\{111\}$, $\{112\}$, and $\{123\}$. There are two valence electron to atom ratios of special interest. First, at $e/a \sim 4.1$ four different moduli vanish simultaneously (E_{001} , E_{011} , G_{011} , and G_{111}): the bcc lattice becomes unstable in the absence of an applied stress. The simultaneous vanishing of these four moduli signifies a spontaneous bcc to hexagonal-close-packed (hcp) transition as the electron concentration drops.

The second special value is $e/a \sim 4.7$, where the tetragonal shear modulus $C' = (C_{11} - C_{12})/2$ is equal to the shear modulus C_{44} . At this concentration, the alloy is elastically isotropic. The alloy becomes increasingly anisotropic as the electron concentration falls. When $e/a \sim 4.24$, a typical value for Gum Metal, the Ti-V alloy has very low moduli for $\langle 111 \rangle$ shear and $\langle 001 \rangle$ tension but is highly anisotropic.

The ideal strengths of Ti-V alloys are computed for uniaxial tension in $\langle 001 \rangle$ (the weak direction in bcc) and simple shear in $\{112\}\langle 111 \rangle$ (the weakest slip system) using the methodology described in [11]. The ideal shear stress-strain curves are plotted in Fig. 2(a) for $\text{Ti}_{75}\text{V}_{25}$, $\text{Ti}_{65}\text{V}_{35}$, and $\text{Ti}_{55}\text{V}_{45}$. The stress-strain curves are approximately sinusoidal, a result expected from symmetry, with an initial slope fixed by the modulus (G_{111}) of the relaxed bcc

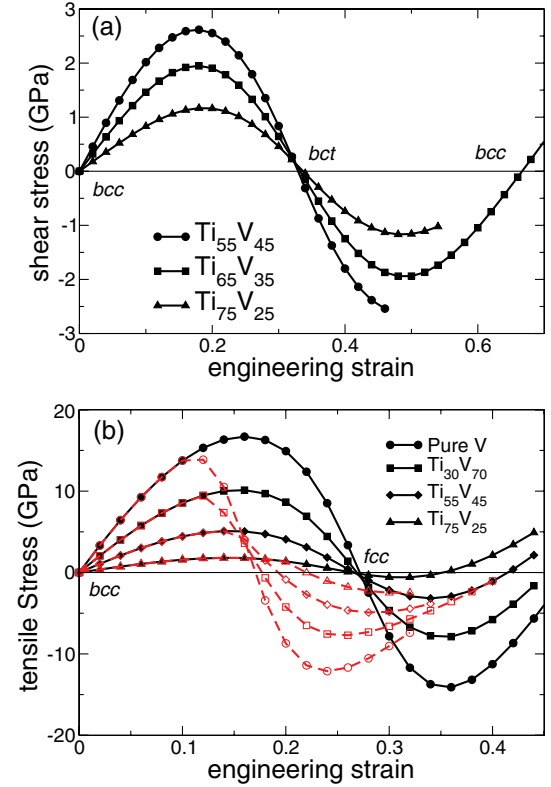


FIG. 2 (color online). (a) Ideal uniaxial shear deformation along $\langle 111 \rangle$ on $\{112\}$ in Ti-V binary bcc alloys. (b) Ideal uniaxial tensile deformation along $\langle 100 \rangle$. The solid and open symbols represent the tetragonal path (Bain path) and orthorhombic path, respectively.

crystal. The ideal shear strength, τ_m —the maximum in the curve—is $\tau_m \sim (\varepsilon_m/\pi)G_{111} = 0.11G_{111}$, where $\varepsilon_m \sim 0.34$ is the strain associated with transformation to a stress-free body-centered tetragonal state (bct). Hence the ideal shear strength scales directly with the shear modulus, and decreases monotonically with e/a . Further, Roundy *et al.* showed that the ideal shear stress for slip on the $\{110\}$ and $\{123\}$ planes of W is nearly equal to the ideal strength for slip on the $\{112\}$ plane [14]. Since bcc symmetry is the origin of this approximate equality, we use the ideal shear strength on the $\{112\}$ plane as representative of shear strength along the other slip planes [24].

A very similar result obtains for a tetragonal strain (the “Bain” path) in uniaxial tension along $\langle 001 \rangle$, the usual weak direction in the bcc structure. The calculated results are presented in the dark curves in Fig. 2(b). A tetragonal strain of ~ 0.28 in the $[001]$ direction transforms the bcc lattice into face-centered-cubic (fcc) (this is the “Bain strain” that governs martensitic transformations in steel [25]). Since the fcc structure is also stress-free (by symmetry), the ideal tensile strength is reached at a tensile strain of about 0.14, at a tensile stress $\sigma_m \sim 0.09E_{001}$. The tensile strength decreases monotonically with E_{001} , and consequently, with e/a .

Given that both G_{111} and E_{001} decrease monotonically with e/a , it is not surprising that Ti-V alloys have relatively low ideal strengths as the concentration draws close to bcc-hcp transition. Interestingly, the calculated ideal tensile strength of $\text{Ti}_{75}\text{V}_{25}$, an alloy with an e/a very close to that of Gum Metal, is comparable to the measured strength of Gum Metal [16]: 1.8 GPa at 0 K (calculated) vs 1.8 GPa at 77 K (measured).

However, if the tensile behavior of Gum Metal were like that shown by the solid curves in Fig. 2(b) the alloy would be brittle: The failure that intrudes on the tetragonal, Bain strain path of a bcc crystal is in tension perpendicular to $\{001\}$, and leads to the conventional $\{001\}$ cleavage of bcc metals [25]. But there is a second possible failure mechanism for a bcc metal at its ideal strength in tension [10]: a bcc metal may also fail by shear on planes that are angled to $[001]$. If a bcc metal is to be ductile at its ideal strength, it must fail in this alternate mode. As illustrated by the dashed curves in Fig. 2(b), a bcc crystal that is strained infinitesimally in the $[001]$ direction in tension follows the Bain path, with equal Poisson contractions in the $[010]$ and $[100]$ directions. However, finite strain may result in a deviation onto an orthorhombic strain path with different perpendicular Poisson contractions. If the strain path branches onto the orthorhombic path before the maximum stress is reached, then the failure will ordinarily be in shear [10]. Thus Ti-V alloys with less than 0.55 Ti ($e/a > 4.45$) fail in shear when pulled in tension.

A useful alternative interpretation of shear failure at the ideal strength can be based on the thermomechanical criteria that govern elastic stability [5]. The limit of elastic stability is reached when the least eigenvalue of the tensor of effective elastic constants vanishes (the Wallace tensor). The eigenvector conjugate to this eigenvalue determines the direction of the failure in configuration space, i.e., the mode of failure. In the present case examination of the eigen solutions indicates that the failure mode is determined by the relative magnitudes of two elastic constants. Specifically, when $G_{001} < E_{001}$, the material fails in shear even when pulled in tension.

Interestingly, the binary Ti-V alloy that is closest to Gum Metal, $\text{Ti}_{75}\text{V}_{25}$, is predicted to fail in tension, and is, therefore, not ideal. However, Gum Metal alloys are rich in Nb, rather than V. The elastic constants of $\text{Ti}_{75}\text{Nb}_{25}$ have been computed using a supercell method [22]. The predicted value of C_{44} ($= 14.9$ GPa) is considerably smaller than E_{001} ($= 19.2$ GPa), indicating that Gum Metal alloys are intrinsically ductile.

While these results clarify why Gum Metal fails in a ductile mode at a moderate value of the ideal strength, we still must understand why Gum Metal is so resistant to deformation by dislocations.

Saito *et al.* report that the solute hardening effect of oxygen, perhaps in the form of ZrO clusters [16], enables the unique mechanical properties of Gum Metal to emerge

[18]. Consider, then, dislocation glide through a random distribution of obstacles [26]. The critical resolved shear stress τ_c for dislocation glide is [26]

$$\tau_c = \alpha \left[\frac{2T}{lb} \right] \beta_c^{3/2} \quad (1)$$

where T is the line tension of the dislocation, l is the mean distance between obstacles in the glide plane, b is the Burgers' vector of the dislocation, (β_c is the dimensionless strength of the obstacles, and α is a geometry dependent prefactor ($\alpha \sim 0.9$ for randomly distributed obstacles). Assuming the obstacles to be impenetrable yields $\beta_c \sim 0.7$, and writing the line tension in the form $T = Kb^2/2$, we have

$$\tau_c \approx 0.53 \left[\frac{K}{l^*} \right], \quad (2)$$

where l^* is the dimensionless obstacle spacing (l/b), and K is the elastic energy factor for the dislocation.

If the resolved stress to move dislocations exceeds the ideal shear strength of the material, dislocations will not mediate plasticity. Dislocation mediated plasticity of bcc metals and alloys is often controlled by the mobility of dislocations in the $\{112\}$, $\{110\}$, and $\{123\}$ planes. As mentioned above, the ideal shear strength for shears in a $\langle 111 \rangle$ direction parallel to the $\{112\}$ plane is given by $\tau_m = 0.11G_{111}$, and this ideal strength is representative for the ideal strength along the other potential slip planes. Thus dislocation motion will not be possible if

$$0.11G_{111} \leq 0.53 \left[\frac{K}{l^*} \right] \quad \text{or} \quad l^* \leq 4.8 \frac{K}{G_{111}} \equiv l_c^*. \quad (3)$$

Here, l_c^* is defined as the dimensionless critical pinning length. If the average (dimensionless) obstacle spacing in the crystal is less than l_c^* , the dislocations will be pinned.

The low-temperature deformation of bcc metals is controlled by the mobility of screw dislocations. The line tension of a $\langle 111 \rangle$ screw dislocation was computed by Head [27] employing the theory of Stroh [28]. Using this

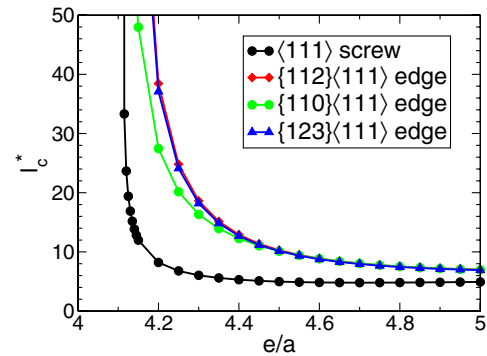


FIG. 3 (color online). The dimensionless pinning lengths for the indicated dislocations plotted as a function of the electron to atom ratio.

result, one finds that

$$\frac{K_{111}^{\text{screw}}}{G_{111}} \propto \frac{1}{\sqrt{C_{11} - C_{12}}}, \quad (4)$$

and

$$\frac{K}{G_{111}} \propto (C_{11} - C_{12})^{-1} \quad (5)$$

for all the candidate nonscrew dislocations. Since $C_{11} - C_{12} \rightarrow 0$ as e/a approaches the value associated with the bcc to hcp transition, l_c^* diverges. Figure 3 plots computed values of l_c^* as a function of e/a for the $\langle 111 \rangle$ screw dislocation, and the edge dislocations in the $\{112\}$, $\{110\}$ and $\{123\}$ slip planes. The l_c^* values for all of the considered dislocations lie above the curve plotted for the $\langle 111 \rangle$ screw dislocation.

The critical lengths plotted in Fig. 3 are insightful. The divergence insures that for e/a sufficiently close the transition, one can introduce an obstacle density sufficient to pin all dislocations, before the ideal shear strength of the material drops to zero. Thus the tuning of the e/a ratio of an intrinsically ductile alloy to be near the bcc to hcp transition leads to a ductile material that is sufficiently elastically anisotropic that one can introduce alloying additions to pin the dislocations and suppress conventional-dislocation mediated deformation.

This explanation of Gum Metal behavior presents several exciting opportunities for materials theorists and metallurgists. First and foremost, since the mechanical properties of these materials are linked to quantities that can be computed directly using the best available quantum mechanical based total energy methods, there is a genuine opportunity for rapid, computer aided, advanced engineering of these alloys. Second, the explanation identifies the bcc to hcp transition as a metallurgically useful transition. Third, the criteria suggest how theory can be used to identify other candidates for Gum Metal behavior: one simply needs to compute the elastic constants and ideal strengths of bcc/hcp alloys as a function of composition.

The authors acknowledge insightful discussions with Dr. Naoki Nakamura of Toyota Motor Corporation. T.L., J.W.M., and D.C.C. gratefully acknowledge the support of Toyota Research and Development and the National Science Foundation under Grant No. DMR 0304629.

*Corresponding author.

Electronic address: dcchrzan@berkeley.edu

- [1] J. Frenkel, Z. Phys. **37**, 572 (1926).
- [2] E. Orowan, Z. Phys. **89**, 605 (1934).
- [3] M. Polyani, Z. Phys. **89**, 660 (1934).
- [4] G.I. Taylor, Proc. R. Soc. A **145**, 362 (1934).
- [5] J. W. Morris, Jr. and C. R. Krenn, Philos. Mag. A **80**, 2827 (2000).
- [6] J. W. Morris, Jr., C. R. Krenn, D. Roundy, and Marvin L. Cohen, *Phase Transformations and Evolution in Materials* (TMS, Warrendale, PA, 2000), p. 187.
- [7] J. Li, K. J. V. Vliet, T. Zhu, S. Yip, and S. Suresh, Nature (London) **418**, 307 (2002).
- [8] S.-H. Jhi, S. Louie, M. Cohen, and J. Morris, Phys. Rev. Lett. **87**, 075503 (2001).
- [9] M. Sob, L. Wang, and V. Vitek, Kovove Materialy **36**, 145 (1998).
- [10] Weidong Luo, D. Roundy, Marvin L. Cohen, and J. W. Morris, Jr., Phys. Rev. B **66**, 094110 (2002).
- [11] Tianshu Li, J.W. Morris, Jr., and D.C. Chrzan, Phys. Rev. B **70**, 054107 (2004).
- [12] D. M. Clatterbuck, C. R. Krenn, M. L. Cohen, and J. W. Morris, Jr., Phys. Rev. Lett. **91**, 135501 (2003).
- [13] D. M. Clatterbuck, D. C. Chrzan, and J. W. Morris, Jr., Scr. Mater. **49**, 1007 (2003).
- [14] D. Roundy, C. R. Krenn, Marvin L. Cohen, and J. W. Morris, Jr., Philos. Mag. A **81**, 1725 (2001).
- [15] C. R. Krenn, D. Roundy, M. L. Cohen, D. C. Chrzan, and J. J. W. Morris, Phys. Rev. B **65**, 134111 (2002).
- [16] T. Saito, T. Furuta, J.-H. Hwang, S. Kuramoto, K. Nishino, N. Suzuki, R. Chen, A. Yamada, Y. Seno, and T. Nonaka *et al.*, Science **300**, 464 (2003).
- [17] M. Y. Gutkin, T. Ishizaki, S. Kuramoto, and I. A. Ovid'ko, Acta Mater. **54**, 2489 (2006).
- [18] T. Saito, T. Furuta, J.-H. Hwang, S. Kuramoto, K. Nishino, N. Suzuki, R. Chen, A. Yamada, K. Ito, Y. Seno, T. Nonaka, H. Ikehata, N. Nagasako, C. Iwamoto, Y. Ikuhara, and T. Sakuma, Mater. Sci. Forum **426-432**, 681 (2003).
- [19] P. Souvatzis, M. I. Katsnelson, S. Simak, R. Ahuja, O. Eriksson, and P. Mohn, Phys. Rev. B **70**, 012201 (2004).
- [20] X. Gonze, J.-M. Beuken, R. Caracas, F. Detraux, M. Fuchs, G.-M. Rignanese, L. Sindic, M. Verstraete, G. Zerah, and F. Jollet *et al.*, Comput. Mater. Sci. **25**, 478 (2002).
- [21] M. Fuchs and M. Scheffler, Comput. Phys. Commun. **119**, 67 (1999).
- [22] H. Ikehata, N. Nagasako, T. Furuta, A. Fukumoto, K. Miwa, and T. Saito, Phys. Rev. B **70**, 174113 (2004).
- [23] K. W. Katahara, M. H. Manghnan, and E. S. Fisher, J. Phys. F **9**, 773 (1979).
- [24] Computed ideal strengths along the other potential slip planes for the $\text{Ti}_{75}\text{V}_{25}$ alloy are within 0.25 GPa of the representative value.
- [25] F. Milstein, in *Mechanics of Solids*, edited by H. Hopkins and M. Sewell (Pergamon, Oxford, 1982), p. 417.
- [26] K. Hansen and J. W. Morris, Jr., J. Appl. Phys. **46**, 983 (1975).
- [27] A. K. Head, Phys. Status Solidi **6**, 461 (1964).
- [28] A. N. Stroh, Philos. Mag. **3**, 625 (1958).